

# Soft-gluon effects in $WW$ production at hadron colliders

Massimiliano Grazzini

INFN, Sezione di Firenze  
and Dipartimento di Fisica, Università di Firenze,  
I-50019 Sesto Fiorentino, Florence, Italy

## Abstract

We consider QCD radiative corrections to  $WW$  pair production in hadron collisions. We perform a calculation that consistently combines next-to-leading order predictions with soft-gluon resummation valid at small transverse momenta  $p_T^{WW}$  of the  $WW$  pair. We present results for the  $p_T^{WW}$  distribution at the LHC up to (almost) next-to-next-to-leading logarithmic accuracy, and study the effect of resummation on the charged-lepton distributions. Soft-gluon effects are typically mild, but they can be strongly enhanced when hard cuts are applied. The relevant distributions are generally well described by the MC@NLO event generator.

# 1 Introduction

Vector boson pair production in hadron collisions is important for physics within and beyond the Standard Model (SM). First of all, this process can be used to measure the vector boson trilinear couplings. Any deviation from the pattern predicted by  $SU(2) \otimes U(1)$  gauge invariance would be a signal of new physics. The Tevatron collaborations are currently measuring  $WW$ ,  $WZ$  and  $W\gamma$  cross sections at invariant masses larger than those probed at LEP2, setting limits on the corresponding anomalous couplings [1].

Furthermore, vector boson pairs are an important background for new physics searches. If a heavy enough Higgs boson does exist, it will decay with large branching ratios in  $WW$  and  $ZZ$  pairs, whereas charged Higgs bosons from non standard Higgs sectors may decay into  $WZ$  final states [2]. Typical signals of supersymmetry, e.g. three charged leptons plus missing energy, find an important background in  $WZ$  and  $W\gamma$  production [3].

In this context,  $WW$  production has received considerable attention. This process provides an irreducible background to the Higgs boson search in the  $H \rightarrow WW \rightarrow l\nu l\nu$  channel, which is the most important when the mass  $M_H$  of the Higgs boson is in the range  $155 \lesssim M_H \lesssim 170$  GeV. Since two neutrinos are present in the final state, no invariant-mass peak can be reconstructed. Fortunately, the angular correlations among the charged leptons suggest a good discrimination of the signal over the background [4], provided the background can be reliably extrapolated into the signal region. It is thus essential to have good control on the SM prediction for the  $WW$  cross section as well as for the associated distributions.

QCD corrections to  $WW$  production at next-to-leading-order (NLO) have been computed more than 10 years ago [5, 6] and enhance the cross section by about 40% at LHC energies. These calculations were done with the traditional method of evaluating directly the relevant squared amplitudes. As a consequence, the  $W$ 's polarization was summed over and spin correlations were not taken into account.

More recent NLO calculations exist that, using the one-loop helicity amplitudes computed in Ref. [7], fully take into account spin correlations [8]. The general purpose NLO program MCFM [9] includes in addition single-resonant contributions neglected in the calculation of Ref. [8]. Very recently, the effect of the potentially large next-to-next-to-leading (NNLO) contribution from the one-loop  $gg \rightarrow WW \rightarrow l\nu l\nu$  diagrams has also been studied [10, 11].

The fixed-order NLO calculations provide a reliable estimate of  $WW$  cross sections and distributions as long as the scales involved in the process are all of the same order. When the transverse momentum of the  $WW$  pair  $p_T^{WW}$  is much smaller than its invariant mass  $M_{WW}$  the validity of the fixed-order expansion may be spoiled since the coefficients of the perturbative expansion can be enhanced by powers of the large logarithmic terms,  $\ln^n M_{WW}/p_T^{WW}$ . This is certainly the case for the  $p_T^{WW}$  spectrum, which, when evaluated at fixed order, is even divergent as  $p_T^{WW} \rightarrow 0$ , and thus requires an all-order resummation of the logarithmically enhanced terms. Resummation effects, however, can be visible also in other observables, making it important to study them in detail.

The way to perform transverse-momentum resummation is known [12]-[20]: to correctly implement momentum conservation in the transverse plane the resummation has to be performed in impact parameter  $b$ -space,  $b$  being the variable conjugated to  $p_T$  through a Fourier transformation.

In the case of vector boson pair production, transverse-momentum resummation has been applied to  $\gamma\gamma$  [21] and  $ZZ$  [22] pair production. To our knowledge, the case of  $WW$  pair production has not been considered yet.

In the present paper we report on an implementation of  $b$ -space resummation to  $WW$  production in hadron collisions. We use the helicity amplitudes of Ref. [7] and work in the narrow width approximation (i.e. we only consider double-resonant contributions), but fully include the decay of the  $W$ 's, keeping track of their polarization in the leptonic decay. In the large  $p_T^{WW}$  region we use LO perturbation theory ( $WW+1$  parton); in the region  $p_T^{WW} \ll M_{WW}$  the large logarithmic contributions are resummed to (almost) next-to-next-to-leading logarithmic (NNLL) [23, 24] accuracy. Our results have thus uniform NLO accuracy but consistently include the effect of resummation in the region  $p_T^{WW} \ll M_{WW}$ .

To perform the resummation we use the formalism of Refs. [25, 26]. In this approach, the resummation is achieved at the level of the partonic cross section and the large logarithmic contributions are exponentiated in a process-independent manner, being constrained to give vanishing contribution to the total cross section.

Besides computing transverse momentum spectra of the  $WW$  pair, we study the effect of resummation on the leptonic distributions, when different cuts are applied. We also compare our results with those obtained at NLO and with the ones from the general purpose event generator MC@NLO [27], which, in its latest release [28], partially includes the effect of spin correlations in the  $W$ 's decay.

The paper is organized as follows. In Sect. 2 we discuss the application of  $b$ -space resummation to  $WW$  production. In Sect. 3 we present our numerical results and in Sect. 4 we draw our conclusions.

Preliminary results of this work for the  $p_T^{WW}$  spectrum were used in the study of Ref. [29].

## 2 Transverse-momentum resummation for $WW$ pair production

In this Section we apply  $b$ -space resummation to the production of  $WW$  pairs in hadron collisions. The resummation formalism we use is completely general, and, as discussed in detail in Ref. [26], can be applied to a generic process in which a system of non strongly interacting particles of high mass  $M$  is produced in hadronic collisions. In the case of  $WW$  production, the mass  $M$  is the invariant mass of the  $WW$  system.

The resummation is performed at the level of the partonic cross section, which is decomposed as:

$$\frac{d\hat{\sigma}_{WW\,ab}}{dM^2 dp_T^2} = \frac{d\hat{\sigma}_{WW\,ab}^{(\text{res.})}}{dM^2 dp_T^2} + \frac{d\hat{\sigma}_{WW\,ab}^{(\text{fin.})}}{dM^2 dp_T^2}. \quad (1)$$

The first term on the right hand side,  $d\hat{\sigma}_{WW\,ab}^{(\text{res.})}$ , contains all the logarithmically enhanced contributions at small  $p_T$ , and has to be evaluated by resumming them to all orders in  $\alpha_S$ . The

second term,  $d\hat{\sigma}_{WW\,ab}^{(\text{fin.})}$ , is free of such contributions, and can thus be evaluated at fixed order in perturbation theory.

The resummed component  $d\hat{\sigma}_{WW\,ab}^{(\text{res.})}$  can be expressed as

$$\frac{d\hat{\sigma}_{WW\,ab}^{(\text{res.})}}{dM^2 dp_T^2}(p_T, M, \hat{s}; \alpha_S(\mu_R^2), \mu_R^2, \mu_F^2) = \frac{M^2}{\hat{s}} \int_0^\infty db \frac{b}{2} J_0(bp_T) \mathcal{W}_{ab}^{WW}(b, M, \hat{s}; \alpha_S(\mu_R^2), \mu_R^2, \mu_F^2), \quad (2)$$

where  $J_0(x)$  is the 0-order Bessel function,  $\mu_R$  ( $\mu_F$ ) is the renormalization (factorization) scale and  $\hat{s}$  is the partonic centre-of-mass energy. By taking the  $N$ -moments of  $\mathcal{W}$  with respect to the variable  $z = M^2/\hat{s}$  at fixed  $M$  the resummation structure of  $\mathcal{W}_{ab,N}^F$  can indeed be organized in exponential form <sup>†</sup>

$$\mathcal{W}_N^{WW}(b, M; \alpha_S(\mu_R^2), \mu_R^2, \mu_F^2) = \mathcal{H}_N^{WW}(M, \alpha_S(\mu_R^2); M^2/\mu_R^2, M^2/\mu_F^2, M^2/Q^2) \times \exp\{\mathcal{G}_N(\alpha_S(\mu_R^2), L; M^2/\mu_R^2, M^2/Q^2)\}, \quad (3)$$

where we have defined the logarithmic expansion parameter  $L$  as

$$L \equiv \ln \frac{Q^2 b^2}{b_0^2} \quad (4)$$

and the coefficient  $b_0 = 2e^{-\gamma_E}$  ( $\gamma_E = 0.5772\dots$  is the Euler number) has a kinematical origin. The scale  $Q$  appearing in Eqs. (3, 4), named resummation scale in Ref. [26], parametrizes the arbitrariness in the resummation procedure, and has to be chosen of the order of the hard scale  $M$ . Variations of  $Q$  around  $M$  can give an idea of the size of yet uncalculated higher-order logarithmic contributions. The function  $\mathcal{H}_N^{WW}$  does not depend on the impact parameter  $b$  and it includes all the perturbative terms that behave as constants as  $b \rightarrow \infty$ . It can thus be expanded in powers of  $\alpha_S = \alpha_S(\mu_R^2)$ :

$$\mathcal{H}_N^{WW}(M, \alpha_S; M^2/\mu_R^2, M^2/\mu_F^2, M^2/Q^2) = \sigma_{WW}^{(0)}(\alpha_S, M) \left[ 1 + \frac{\alpha_S}{\pi} \mathcal{H}_N^{WW(1)}(M^2/\mu_R^2, M^2/\mu_F^2, M^2/Q^2) + \left(\frac{\alpha_S}{\pi}\right)^2 \mathcal{H}_N^{WW(2)}(M^2/\mu_R^2, M^2/\mu_F^2, M^2/Q^2) + \dots \right] \quad (5)$$

where  $\sigma_{WW}^{(0)}$  is the Born partonic cross section. The exponent  $\mathcal{G}_N$  includes the complete dependence on  $b$  and, in particular, it contains all the terms that order-by-order in  $\alpha_S$  are logarithmically divergent as  $b \rightarrow \infty$ . The logarithmic expansion of  $\mathcal{G}_N$  reads

$$\mathcal{G}_N(\alpha_S(\mu_R^2), L; M^2/\mu_R^2, M^2/Q^2) = Lg^{(1)}(\alpha_S L) + g_N^{(2)}(\alpha_S L; M^2/\mu_R^2, M^2/Q^2) + \frac{\alpha_S}{\pi} g_N^{(3)}(\alpha_S L, M^2/\mu_R^2, M^2/Q^2) + \dots \quad (6)$$

where the term  $Lg^{(1)}$  collects the LL contributions, the function  $g_N^{(2)}$  includes the NLL contributions,  $g_N^{(3)}$  controls the NNLL terms and so forth.

In the implementation of Eq. (3) the resummation of the large logarithmic contributions affects not only the small- $p_T$  region ( $p_T \ll M$ ), but also the region of large  $p_T$  ( $p_T \sim M$ ). This can

---

<sup>†</sup>Here, to simplify the notation, flavour indices are understood, or in other words, we limit ourselves to discussing the flavour non-singlet contribution. A complete discussion of the exponentiation structure in the general case can be found in Appendix A of Ref. [26].

be easily understood by observing that the logarithmic expansion parameter  $L$  is divergent as  $b \rightarrow 0$ . To reduce the impact of unjustified higher-order contributions in the large- $p_T$  region, the logarithmic variable  $L$  in Eq. (4) is replaced as

$$L \rightarrow \tilde{L} \quad \tilde{L} \equiv \ln \left( \frac{Q^2 b^2}{b_0^2} + 1 \right). \quad (7)$$

The variables  $L$  and  $\tilde{L}$  are equivalent when  $Qb \gg 1$ , but they lead to a different behaviour of the form factor at small values of  $b$  (i.e. large values of  $p_T$ ). When  $Qb \ll 1$  in fact,  $\tilde{L} \rightarrow 0$  and  $\exp\{\mathcal{G}_N\} \rightarrow 1$ . The replacement in Eq. (7) has thus a twofold consequence: it reduces the impact of resummation at large values of  $p_T$ , and it allows us to recover the corresponding fixed-order cross section upon integration over  $p_T$ .

Another important property of the formalism of Ref. [26] is that the process dependence (as well as the factorization scale and scheme dependence) is fully encoded in the hard function  $\mathcal{H}^{WW}$ . In other words, the functions  $g^{(i)}$  are universal: they depend only on the channel in which the process occurs at Born level, ( $q\bar{q}$  annihilation in the case of  $WW$  production). Their explicit expressions up to  $i = 3$  are given in Ref. [26] in terms of the universal perturbative coefficients  $A_q^{(1)}$ ,  $A_q^{(2)}$ ,  $A_q^{(3)}$ ,  $\tilde{B}_{q,N}^{(1)}$ ,  $\tilde{B}_{q,N}^{(2)}$ . In particular, the LL function  $g^{(1)}$  depends on the coefficient  $A_q^{(1)}$ , the NLL function  $g_N^{(2)}$  also depends on  $A_q^{(2)}$  and  $\tilde{B}_q^{(1)}$  and the NNLL function  $g_N^{(3)}$  also depends on  $A_q^{(3)}$  and  $\tilde{B}_{q,N}^{(2)}$ . All these coefficients are known except  $A_q^{(3)}$ . In our quantitative study (see Sect. 3) we assume that the value of  $A_q^{(3)}$  is the same as the one [30, 31] that appears in resummed calculations of soft-gluon contributions near partonic threshold.

We now turn to the hard coefficients  $\mathcal{H}_{q\bar{q}\leftarrow ab,N}^{WW}$ . The first order contributions  $\mathcal{H}_{q\bar{q}\leftarrow ab,N}^{WW(1)}$  in Eq. (5) are known. The flavour off-diagonal part is process independent and in the  $\overline{\text{MS}}$  scheme it reads:

$$\mathcal{H}_{q\bar{q}\leftarrow qq,N}^{(1)} = \mathcal{H}_{gg\leftarrow qq,N}^{(1)} = \frac{1}{2(N+1)(N+2)} + \gamma_{qq,N}^{(1)} \ln \frac{Q^2}{\mu_F^2}, \quad (8)$$

where  $\gamma_{ab,N}^{(1)}$  are the LO anomalous dimensions. The flavour diagonal coefficient is instead process dependent, and, as shown in Refs. [23, 24], it can be expressed in terms of the finite part  $\mathcal{A}^{WW \ddagger}$  of the one-loop correction to the Born subprocess, computed in Ref. [7]. We have [26]:

$$\mathcal{H}_{q\bar{q}\leftarrow q\bar{q},N}^{WW(1)} = C_F \left( \frac{1}{N(N+1)} + \frac{\pi^2}{6} \right) + \frac{1}{2} \mathcal{A}^{WW} - \left( B_q^{(1)} + \frac{1}{2} A_q^{(1)} \ln \frac{M^2}{Q^2} \right) \ln \frac{M^2}{Q^2} + 2\gamma_{qq}^{(1)} \ln \frac{Q^2}{\mu_F^2}. \quad (9)$$

The second order coefficients  $\mathcal{H}_{q\bar{q}\leftarrow ab,N}^{WW(2)}$  in Eq. (5) have not yet been computed.

We finally consider the finite component in Eq. (1). This contribution has to be evaluated starting from the usual perturbative truncation of the partonic cross section and subtracting the expansion of the resummed part at the *same* perturbative order. This procedure allows us to combine the resummed and the finite component of the partonic cross section to achieve uniform theoretical accuracy over the entire range of transverse momenta. Note that, since for  $WW$  production at  $p_T^{WW} \neq 0$  only the LO result is known ( $WW+1$  parton), we can perform the matching at LO only.

---

<sup>‡</sup>We adopt here for  $\mathcal{A}^{WW}$  the definition of Eq. (38) of Ref. [24].

In summary, the inclusion of the functions  $g^{(1)}$ ,  $g_N^{(2)}$  and of the coefficient  $\mathcal{H}_N^{WW(1)}$  in the resummed component, together with the evaluation of the finite component at LO, allows us to perform the resummation at NLL+LO accuracy. The inclusion of the function  $g_N^{(3)}$  (still performing the matching at LO) allows us to reach (almost) NNLL+LO accuracy<sup>§</sup>. The reason why we cannot claim full NNLL accuracy is that the NNLL contribution  $\alpha_S g_N^{(3)}$  in the exponent in Eq. (6) is of the same order of the terms coming from the combined effect of  $\alpha_S^2 \mathcal{H}_N^{WW(2)}$  and  $Lg^{(1)}$ , which are not under control. For this reason, in the following Section we will mainly rely on our NLL+LO prediction, regarding the NNLL+LO result as an indication of the size of NNLL effects.

### 3 Results

In this Section we present numerical results for  $WW$  production in  $pp$  collisions at LHC energies. We compare our resummed perturbative predictions at NLL+LO and NNLL+LO accuracy with the NLO ones, obtained with the general purpose program MCFM [9], and with results obtained with the MC@NLO event generator [28].

To compute the  $WW$  cross section we use MRST2002 NLO densities [32] and  $\alpha_S$  evaluated at two-loop order. As discussed in Sect. 2, our resummed predictions depend on renormalization, factorization and resummation scales. Unless stated otherwise, the resummation scale is set equal to the invariant mass  $M_{WW}$  of the  $WW$  pair, whereas renormalization and factorization scales are set to  $2M_W$ . The latter choice allows us to exploit our unitarity constraint and to exactly recover the total NLO cross section when no cuts are applied. At NLO we consistently use  $\mu_F = \mu_R = 2M_W$  as default choice, whereas in MC@NLO  $\mu_F$  and  $\mu_R$  are set to the default choice, the average transverse mass of the  $W$ 's.

The predictions of resummation are implemented in a partonic Monte Carlo program which generate the full 5-body final state ( $l\nu l\nu + 1$  parton). Nonetheless, since the resummed cross section in Eq. (1) is inclusive over rapidity, we are not able to apply the usual rapidity cuts on the leptons<sup>¶</sup>. To the purpose of the present work, we do not expect this limitation to be essential. Note also that, since the resummation formalism we use is valid for the inclusive production of a non-strongly interacting final state ( $WW \rightarrow l\nu l\nu$  in the present case), we are not allowed to apply cuts on the accompanying jets.

We start by considering the inclusive cross sections. Our NLL+LO (NNLL+LO) result is 115.6 (115.5) pb, and agrees with the NLO one (116.0 pb) to better than 1%. The cross section from MC@NLO is instead lower, about 114.7 pb. The above difference is due to the different choice of the scales, and to the different convention in the choice of the electroweak couplings adopted in MC@NLO.

In Fig. 1 (left) we show the corresponding  $p_T$  distribution, computed at NLL+LO (dotted),

---

<sup>§</sup>The reader should not be confused by this notation: the NLL+LO and NNLL+LO results include the complete  $\mathcal{O}(\alpha_S)$  real contribution through the finite component in Eq. (1) as well as the full virtual  $\mathcal{O}(\alpha_S)$  correction through the  $\mathcal{H}_{q\bar{q} \leftarrow q\bar{q}, N}^{WW(1)}$  coefficient in Eq. (9). As a consequence, our NLL+LO and NNLL+LO results contain the complete NLO correction plus resummation of the large logarithmic contributions at  $p_T^{WW} \ll M_{WW}$ .

<sup>¶</sup>Note that this is not a limitation of principle: the resummation formalism can be extended to the double differential transverse momentum and rapidity distribution.

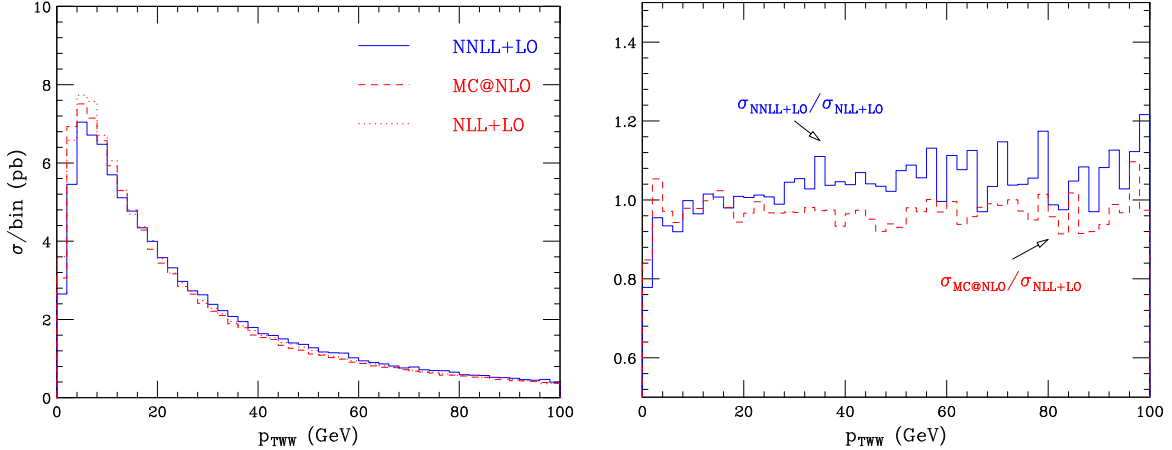


Figure 1: *Left: comparison of the transverse momentum spectra of the  $WW$  pair obtained at NLL+LO, NNLL+LO and with MC@NLO. No cuts are applied. Right: NNLL+LO and MC@NLO results normalized to NLL+LO.*

NNLL+LO (solid) and with MC@NLO (dashed). The NLO result, not shown in the plot, diverges to  $+\infty$  as  $p_T^{WW} \rightarrow 0$ . We see that the three histograms are very close to each other and show a peak around  $p_T^{WW} \sim 5$  GeV. The agreement is confirmed in Fig. 1 (right) where the ratio of the NNLL+LO (solid) and MC@NLO (dashed) results to the NLL+LO are displayed. We see that, apart from statistical fluctuations, the MC@NLO and NLL+LO agree within 2-3 % on average. On the contrary, the NNLL contribution tends to make the distribution harder and its effect increases at higher  $p_T$ , always being below 10%.

In order to study the perturbative uncertainties affecting our NLL+LO calculation, we have varied  $\mu_F$  and  $\mu_R$  by a factor 2 around the central value. We find that the effect of scale variations is rather small, of the order of  $\pm 1\%$ , and comparable with the estimated accuracy of our numerical code. Similar results are obtained by varying  $\mu_F$  and  $\mu_R$  in MC@NLO.

The dependence of our NLL+LO results on the resummation scale is instead stronger. In Fig. 2 we show the NLL+LO prediction for different values of the resummation scale  $Q$ . We see that varying the resummation scale the effect on the  $p_T^{WW}$  spectrum is well visible and amounts to about  $\pm 10\%$  at the peak. For lower (higher) values of  $Q$  the effect of the resummation is confined to smaller (larger) values of  $p_T^{WW}$ . Comparing Figs. 1 and 2 we see that the order of magnitude of the NNLL effect, partially included in our NNLL+LO prediction, is smaller than the spread in the NLL+LO result from resummation-scale variations.

As in the case of Higgs production [26], we find that the choice  $Q = 2M_{WW}$  gives (slightly) negative cross sections at very large  $p_T^{WW}$ . In order to define a range of variation of  $Q$ , we would like to avoid values that give a bad behaviour at large  $p_T^{WW}$ . For this reason in the following we will consider resummation-scale variations in the range  $M_{WW}/4 \leq Q \leq M_{WW}$ .

We now consider the  $p_T$  spectra of the leptons. For each event, we classify the transverse momenta of the two charged leptons into their minimum and maximum values,  $p_{T\min}^l$  and  $p_{T\max}^l$ . In Fig. 3 we plot the corresponding  $p_T$  spectra, computed at NLL+LO (solid), NLO (dotted) and with MC@NLO (dashes). We see that all the three predictions are in good agreement. Small

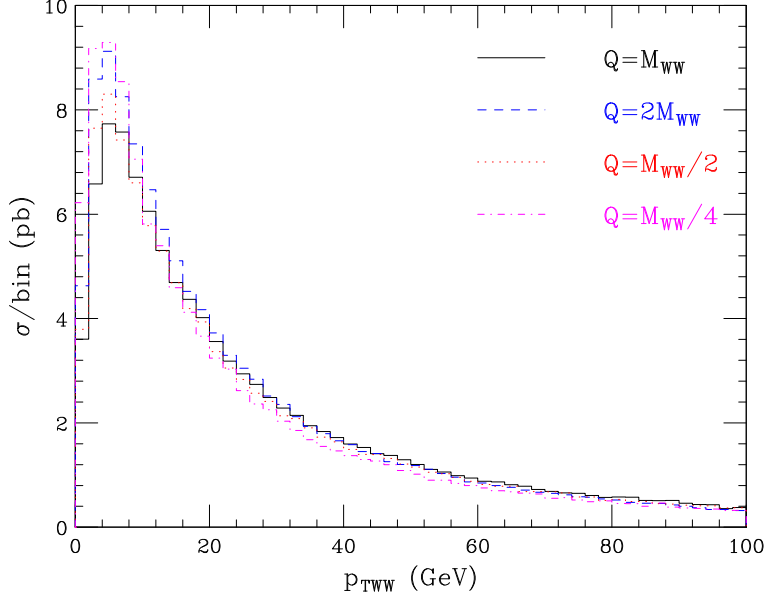


Figure 2: *NLL+LO spectra for different values of the resummation scale  $Q$ .*

differences are visible in the peak of the  $p_T$  distribution of the lepton with larger  $p_T$ : the peak predicted by MC@NLO and by the NLL+LO calculation is slightly lower than the one from the NLO calculation. The renormalization- and factorization-scale dependence of the results, defined as above, is still of about  $\pm 1\%$ . The scale uncertainty of the NLL+LO result is dominated by resummation-scale variations and it is about  $\pm 2 - 3\%$  on average.

We then examine the impact of resummation when cuts on the final state are applied. We start by defining the following selection criteria, taken from the study of Ref. [29].

#### Cuts A:

- The  $p_T$  of the charged leptons should be larger than 20 GeV.
- The invariant mass  $m_{ll}$  of the charged leptons should be smaller than 80 GeV.
- The missing  $p_T$  of the event should be larger than 20 GeV.
- The azimuthal separation  $\Delta\phi$  of the charged leptons in the transverse plane should be smaller than  $135^\circ$ .

These cuts basically select a pair of  $W$ 's, suppressing events with lepton pairs originating from the decay of a  $Z$ . The corresponding NLL+LO cross section is 21.03 pb, about 5% smaller than the NLO result of 22.10 pb. The MC@NLO cross section is instead 21.16 pb. The differences between these results are not unexpected: both the NLL+LO and the MC@NLO calculations enforce a unitarity constraint which ensure the correct NLO normalization is recovered when *total* cross sections are considered. When, as in this case, cuts are applied, higher order effects are present that make NLL+LO and MC@NLO results generally different from NLO.



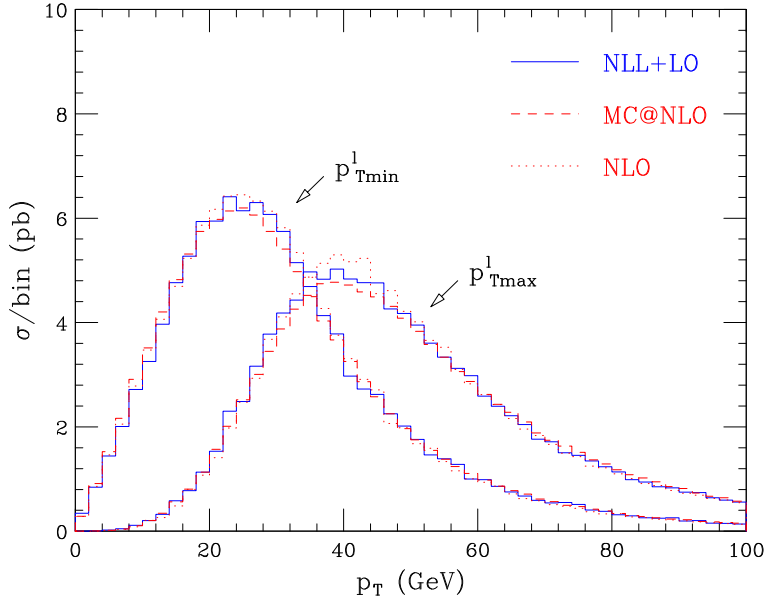


Figure 3: *Distributions in  $p_{T\min}^l$  and  $p_{T\max}^l$ . No cuts are applied.*

In Fig. 4 we show the distributions in  $p_{T\min}^l$  and  $p_{T\max}^l$ : as in Fig. 3, no significant differences are found between the three histograms: these distributions are still reliably predicted by the fixed-order NLO calculation. This conclusion is confirmed by studying scale variations. The effect of renormalization- and factorization-scale variations is still very small, and the impact of resummation-scale variations on the NLL+LO result is again of about  $\pm 2 - 3\%$  on average.

In the search for the Higgs boson in the  $H \rightarrow WW \rightarrow l\nu l\nu$  channel an important difference between the signal and the background is found in the  $\Delta\phi$  distribution. Since the Higgs is a scalar, the charged leptons tend to be produced quite close in angle. As a consequence, the signal is expected to be peaked at small values of  $\Delta\phi$ , whereas the  $\Delta\phi$  distribution for the background is expected to be reasonably flat. It is thus important to study the effect of resummation on this distribution, which is also known to be particularly sensitive to spin correlations [33].

In Fig. 5 the  $\Delta\phi$  distribution at NLL+LO (solid) is compared to the one at NLO (dotted) and from MC@NLO (dashes). The upper panel shows NLL+LO and MC@NLO results normalized to the NLO prediction. Note that both the NLO and the NLL+LO calculations fully include spin correlations, whereas MC@NLO neglects spin correlations in the finite (non factorized) part of the one-loop contribution. We see that the agreement between the three results is excellent, showing that the approximate treatment of spin correlations in MC@NLO is accurate enough. Comparing NLL+LO and MC@NLO predictions with NLO ones we also see that the effects of resummation appear negligible in this situation. As in the case of Fig. 4, this conclusion is confirmed by studying scale variations. The effect of renormalization- and factorization-scale variations is still of about  $\pm 1\%$ . The effect of resummation-scale variations on the NLL+LO prediction, not shown in the plot, is about  $\pm 2\%$ .

We now consider the application of stronger selection criteria [29], designed for the search of a Higgs boson with mass  $M_H = 165$  GeV.

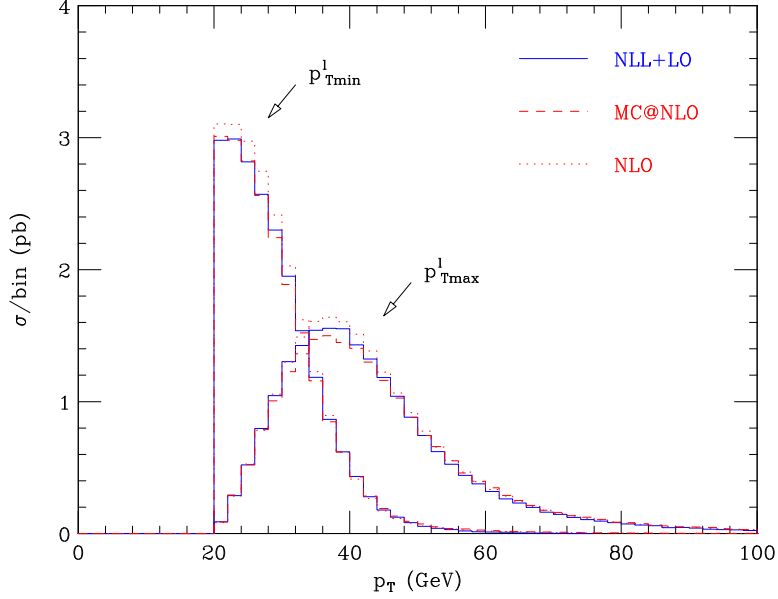


Figure 4: *Distributions in  $p_{T\min}^l$  and  $p_{T\max}^l$ . Cuts A are applied.*

## Cuts B

- For each event,  $p_{T\min}^l$  should be larger than 25 GeV and  $p_{T\max}^l$  should be between 35 and 50 GeV.
- The invariant mass  $m_{ll}$  of the charged leptons should be smaller than 35 GeV.
- The missing  $p_T$  of the event should be larger than 20 GeV.
- The azimuthal separation  $\Delta\phi$  of the charged leptons in the transverse plane should be smaller than  $45^\circ$ .
- A jet veto is mimicked by imposing that the transverse momentum of the  $WW$  pair should be smaller than 30 GeV. This cut is perfectly legitimate in our resummed calculation and is exactly equivalent to a jet veto at NLO.

These cuts further select the small  $\Delta\phi$  region. The jet veto is usually applied in order to reduce the  $t\bar{t}$  contribution, which is expected to produce large- $p_T$   $b$ -jets from the decay of the top quark.

The new cuts reduce the number of  $WW$  events by an additional factor of 35 with respect to cuts A. The NLL+LO (MC@NLO) accepted cross section is 0.599 pb (0.570 pb) which should be contrasted with the NLO result, which is 0.691 pb, about 20% higher. This relative large difference is due to the fact that the new cuts enhance the relevance of the small- $p_T^{WW}$  region, where the NLO calculation is not any more reliable.

In Fig. 6 the  $p_{T\min}^l$  and  $p_{T\max}^l$  distributions are presented. The upper plot shows the two spectra for central values of the scales. We see that although the three predictions are still in reasonable agreement in shape, differences are now evident. In particular, the  $p_{T\min}^l$  distribution at NLO is

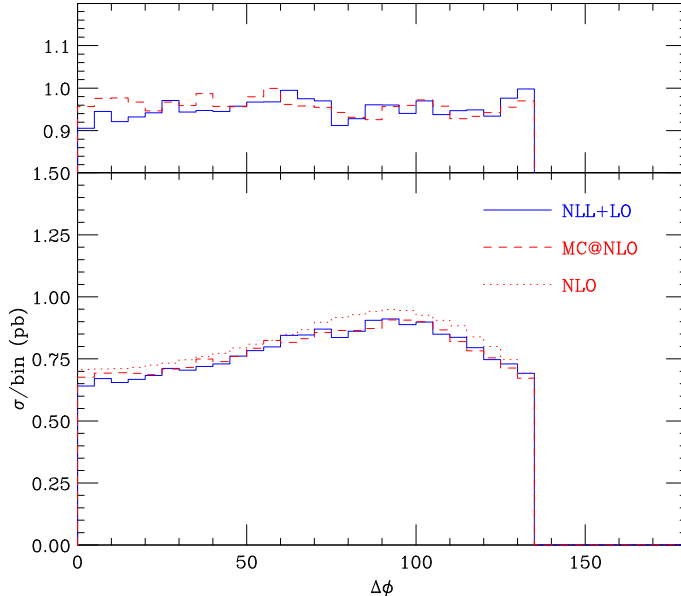


Figure 5: The  $\Delta\phi$  distribution when cuts  $A$  are applied. The upper part of the plot shows the NLL+LO and MC@NLO results normalized to the NLO one.

definitely steeper than the other two. Comparing NLL+LO and MC@NLO spectra, we see that the former are steeper than the latter: with the application of stronger cuts the differences between NLL+LO and MC@NLO predictions are clearly amplified. The lower plot shows the uncertainty band at NLO and NLL+LO. At NLO the band is obtained by varying  $\mu_F = \mu_R$  between  $M_W$  and  $4M_W$ : the effect of scale variations is now more visible and is of the order of a few percent. The corresponding scale variations have marginal effect on the NLL+LO and MC@NLO results: this means that when the small  $p_T^{WW}$  region is selected, scale uncertainties increase at fixed order, while remaining small when resummation is included. At NLL+LO the band is obtained as before by varying the resummation scale  $Q$  between  $M_{WW}$  and  $4M_{WW}$ , and the effect is of about  $\pm 3 - 4\%$ .

In Fig. 7 (left) the  $\Delta\phi$  distribution is displayed. The NLO and NLL+LO bands (right), computed as in Fig. 6, are also shown. We see that the shapes of the three results are still in good agreement with each other, although a slightly different slope of the NLL+LO result with respect to MC@NLO and NLO ones starts to appear.

We finally consider the transverse-mass distribution of the  $WW$  system. We choose to define the transverse mass according to Ref. [34]. We start from the transverse energy of the charged leptons and of the neutrinos, which are expressed as

$$E_{Tu} = \sqrt{p_{Tu}^2 + m_u^2} \quad \cancel{E}_T = \sqrt{\cancel{p}_T^2 + m_{\nu\nu}^2}, \quad (10)$$

where  $\mathbf{p}_{Tu}$  and  $\cancel{\mathbf{p}}_T$  are the total transverse momentum of the charged leptons and the missing transverse momentum, respectively. If the Higgs boson mass is close to the  $WW$  threshold, the invariant mass of the neutrinos in the expression of  $\cancel{E}_T$  can be approximated by  $m_u$  and we can define

$$M_{TWW} = \sqrt{(\cancel{E}_T + E_{Tu})^2 - (\mathbf{p}_{Tu} + \cancel{\mathbf{p}}_T)^2}. \quad (11)$$

In Fig. 8 (left) we show the transverse-mass distribution defined above, computed at NLO

(dotted), NLL+LO (solid) and with MC@NLO (dashes). The inset plot shows the NLO and MC@NLO results normalized to NLL+LO. The plot on the right shows the uncertainty bands computed as in Figs. 6,7. All the three histograms are peaked at  $M_{TWW}$  between 140 and 150 GeV. Comparing the shapes of the histograms, we see that at NLO the shape is fairly different with respect to NLL+LO and MC@NLO. The NLL+LO and MC@NLO distributions also show small differences: the NLL+LO result is steeper and softer than the MC@NLO one.

## 4 Summary

In this paper we studied the effects of soft-gluon resummation in  $WW$  pair production in hadron collisions. We performed a calculation that, using the helicity amplitudes computed in Ref. [7], achieves uniform NLO accuracy over the whole phase space but consistently includes the resummation of the large logarithmic contributions at  $p_T^{WW} \ll M_{WW}$ . We presented predictions for the  $p_T^{WW}$  spectrum at NLL+LO and (almost) NNLL+LO accuracy, and compared our results with those obtained with the MC@NLO event generator, finding good agreement.

We then examined a few charged-lepton distributions: the  $p_T$  spectrum of the lepton with minimum and maximum  $p_T$ , the azimuthal separation of the charged leptons in the transverse plane and the transverse-mass distribution, when different sets of cuts are applied. The  $p_T$  spectra of the charged leptons are generally well described by the NLO calculation but the effect of resummation becomes visible when hard cuts are applied. The  $\Delta\phi$  distribution is important to discriminate a Higgs-boson signal over the background in the  $H \rightarrow WW \rightarrow l\nu l\nu$  channel, and is also known to be particularly sensitive to the effect of spin correlations in the  $W$ 's decay. The latter are fully taken into account at NLO and in our NLL+LO calculation, whereas MC@NLO neglects spin correlations in the finite (non-factorized) part of the one-loop contribution. All the predictions for the  $\Delta\phi$  distribution agree well and resummation effects appear small even when hard cuts are applied. We also examined the transverse mass distribution of the  $WW$  pair. The shape of the NLO distribution differs substantially from NLL+LO and MC@NLO. On the other hand, the NLL+LO and MC@NLO results are still in reasonable agreement.

We finally note that the resummed predictions presented in this paper were obtained in a purely perturbative framework. Two kinds of non-perturbative effects may be considered: those due to hadronization, and those due to an intrinsic transverse momentum (intrinsic  $p_T$ ) of the partons in the colliding hadrons.

In the present paper we were mainly concerned with leptonic observables. As a consequence, we do not expect hadronization effects to be particularly relevant. This expectation is supported by the good agreement we find between resummed results and MC@NLO predictions, in which hadronization effects *are* taken into account.

As far as intrinsic- $p_T$  effects are concerned, it is known (see e.g. Ref. [16] and references therein) that transverse-momentum distributions are affected by such kind of non-perturbative effects, particularly at small transverse momenta. These effects, associated to the large- $b$  region in impact parameter, are not taken into account in our calculation. As noted in Ref. [26], these non-perturbative effects have the same qualitative impact as the inclusion of higher-order logarithmic contributions, i.e., they tend to make the  $p_T$  distribution harder. The precise quantification of

non-perturbative effects in  $WW$  production is left for future investigations.

## Acknowledgements

I wish to thank Stefano Catani for valuable discussions and comments. I also thank Daniel de Florian, Gunther Dissertori, Michael Dittmar, Volker Drollinger, Stefano Frixione, and Zoltan Kunszt for helpful discussions and suggestions, and CERN Theory Unit for the hospitality and financial support at various stages of this work.

## References

- [1] V. D. Elvira [CDF and D0 Collaborations], FERMILAB-CONF-05-329-CD, presented at “19th Rencontres de Physique de la Vallée d’Aoste: Results and Perspectives in Particle Physics”, La Thuile, Aosta Valley, Italy, 27 Feb - 5 Mar 2005.
- [2] See e.g. J. F. Gunion, H. E. Haber, G. L. Kane and S. Dawson, *The Higgs Hunter’s Guide* (Addison-Wesley, Reading, Mass., 1990).
- [3] S. P. Martin, in *Perspectives in Supersymmetry*, edited by G.L. Kane (World Scientific, Singapore, 1998), hep-ph/9709356.
- [4] M. Dittmar and H. K. Dreiner, Phys. Rev. D **55** (1997) 167.
- [5] J. Ohnemus, Phys. Rev. D **44** (1991) 1403.
- [6] S. Frixione, Nucl. Phys. B **410** (1993) 280.
- [7] L. J. Dixon, Z. Kunszt and A. Signer, Nucl. Phys. B **531** (1998) 3.
- [8] L. J. Dixon, Z. Kunszt and A. Signer, Phys. Rev. D **60** (1999) 114037.
- [9] J. M. Campbell and R. K. Ellis, Phys. Rev. D **60** (1999) 113006.
- [10] T. Binoth, M. Ciccolini, N. Kauer and M. Kramer, JHEP **0503** (2005) 065.
- [11] M. Duhrssen, K. Jakobs, J. J. van der Bij and P. Marquard, JHEP **0505** (2005) 064.
- [12] Y. L. Dokshitzer, D. Diakonov and S. I. Troian, Phys. Rep. **58** (1980) 269.
- [13] G. Parisi and R. Petronzio, Nucl. Phys. B **154** (1979) 427.
- [14] G. Curci, M. Greco and Y. Srivastava, Nucl. Phys. B **159** (1979) 451.
- [15] J. C. Collins and D. E. Soper, Nucl. Phys. B **193** (1981) 381 [Erratum-ibid. B **213** (1983) 545].
- [16] J. C. Collins and D. E. Soper, Nucl. Phys. B **197** (1982) 446.
- [17] J. Kodaira and L. Trentadue, Phys. Lett. B **112** (1982) 66, report SLAC-PUB-2934 (1982), Phys. Lett. B **123** (1983) 335.
- [18] G. Altarelli, R. K. Ellis, M. Greco and G. Martinelli, Nucl. Phys. B **246** (1984) 12.

- [19] J. C. Collins, D. E. Soper and G. Sterman, Nucl. Phys. B **250** (1985) 199.
- [20] S. Catani, D. de Florian and M. Grazzini, Nucl. Phys. B **596** (2001) 299.
- [21] C. Balazs, E. L. Berger, S. Mrenna and C. P. Yuan, Phys. Rev. D **57** (1998) 6934.
- [22] C. Balazs and C. P. Yuan, Phys. Rev. D **59** (1999) 114007 [Erratum-ibid. D **63** (2001) 059902].
- [23] D. de Florian and M. Grazzini, Phys. Rev. Lett. **85** (2000) 4678.
- [24] D. de Florian and M. Grazzini, Nucl. Phys. B **616** (2001) 247.
- [25] G. Bozzi, S. Catani, D. de Florian and M. Grazzini, Phys. Lett. B **564** (2003) 65
- [26] G. Bozzi, S. Catani, D. de Florian and M. Grazzini, preprint LPSC 05–63, hep-ph/0508068.
- [27] S. Frixione and B. R. Webber, JHEP **0206** (2002) 029; S. Frixione, P. Nason and B. R. Webber, JHEP **0308** (2003) 007.
- [28] S. Frixione and B. R. Webber, hep-ph/0506182.
- [29] G. Davatz, G. Dissertori, M. Dittmar, M. Grazzini and F. Pauss, JHEP **0405** (2004) 009.
- [30] A. Vogt, Phys. Lett. B **497** (2001) 228; C. F. Berger, Phys. Rev. D **66** (2002) 116002.
- [31] S. Moch, J. A. M. Vermaseren and A. Vogt, Nucl. Phys. B **688** (2004) 101, Nucl. Phys. B **691** (2004) 129.
- [32] A. D. Martin, R. G. Roberts, W. J. Stirling and R. S. Thorne, Eur. Phys. J. C **28** (2003) 455.
- [33] See e.g. T. Gleisberg, F. Krauss, A. Schalicke, S. Schumann and J. C. Winter, Phys. Rev. D **72** (2005) 034028.
- [34] D. L. Rainwater and D. Zeppenfeld, Phys. Rev. D **60** (1999) 113004 [Erratum-ibid. D **61** (2000) 099901].

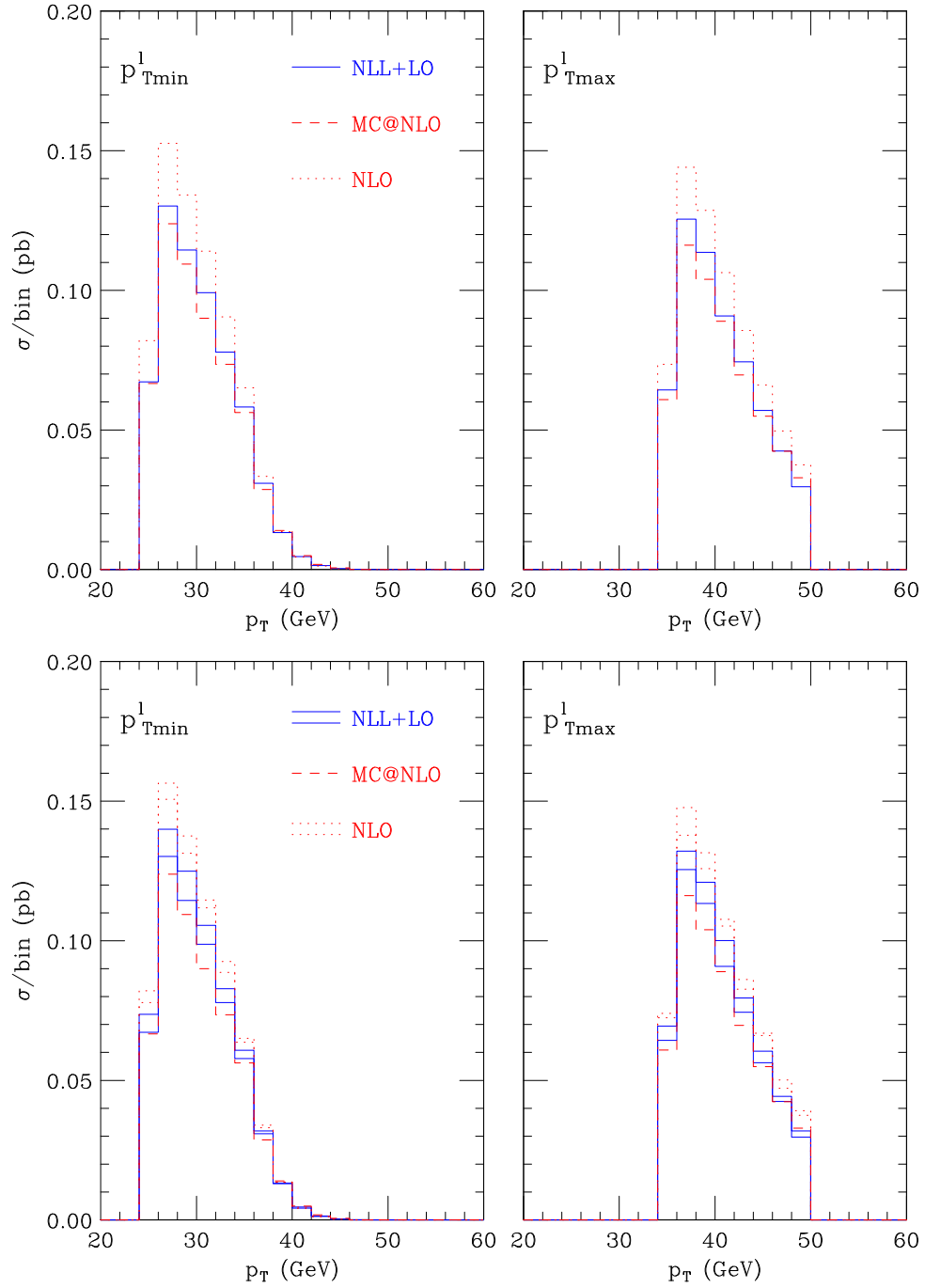


Figure 6: Distributions in  $p_{T\min}^l$  and  $p_{T\max}^l$  when cuts  $B$  are applied. In the lower plot the perturbative uncertainty bands at NLO and NLL+LO are shown.

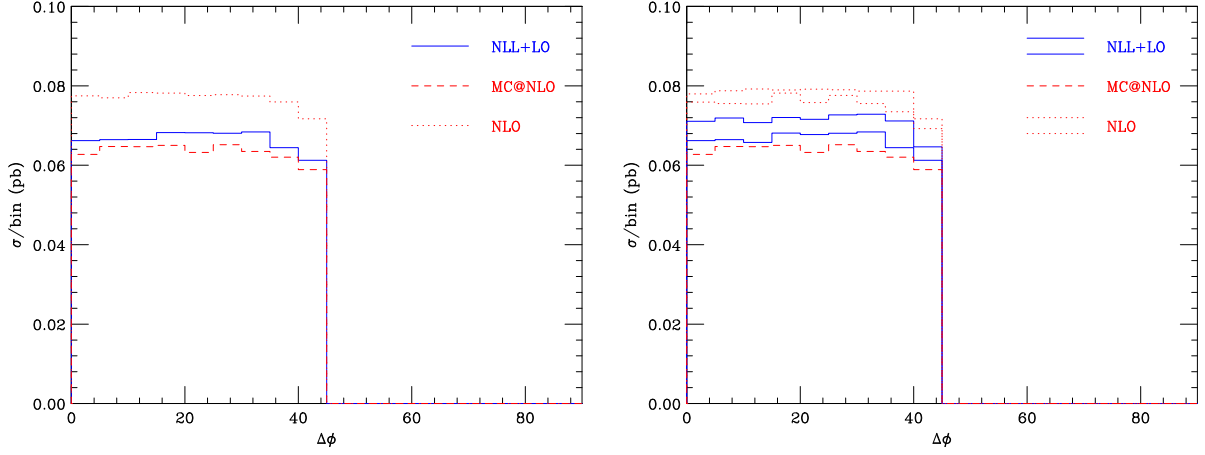


Figure 7: *Left:  $\Delta\phi$  distribution when cuts  $B$  are applied. Right: the corresponding NLL+LO and NLO uncertainty bands are shown.*

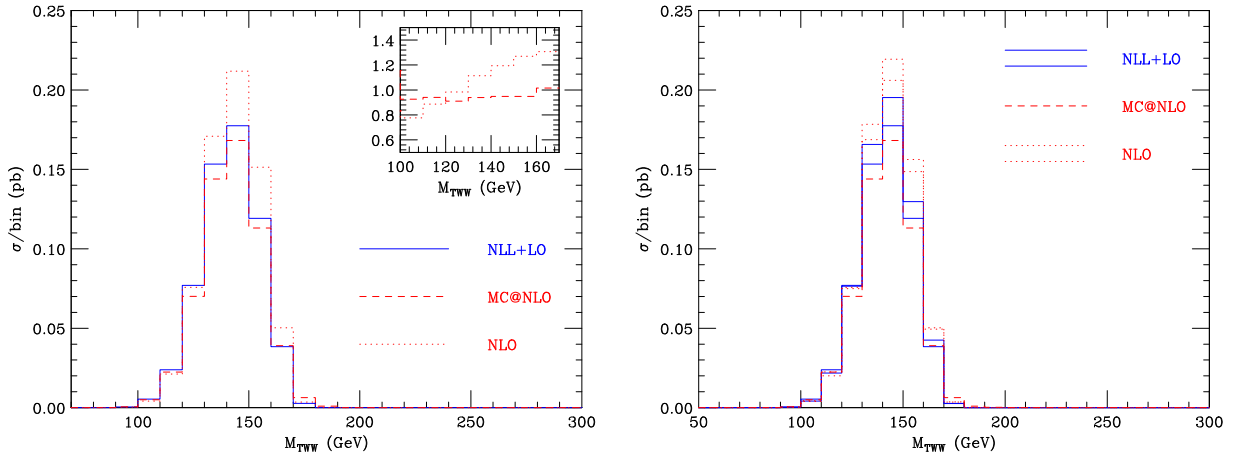


Figure 8: *Left:  $M_{TWW}$  distribution when cuts  $B$  are applied. The inset plot shows NLO and MC@NLO results normalized to NLL+LO. Right: NLL+LO and NLO uncertainty bands computed as in Fig. 7.*